ELSEVIER

Journal of Nuclear Materials 279 (2000) 65–76

journal of nuclear materials

www.elsevier.nl/locate/jnucmat

A comparative evaluation of welding consumables for dissimilar welds between 316LN austenitic stainless steel and Alloy 800

M. Sireesha [a], Shaju K. Albert [b], V. Shankar [b], S. Sundaresan [a,*]

[a] *Department of Metallurgical Engineering, Indian Institute of Technology, Chennai 600 036, India*
[b] *Materials Technology Division, Indira Gandhi Centre for Atomic Research, Kalpakkam 603 102, India*

Received 4 June 1999; accepted 5 November 1999

Abstract

Transition joints in power plants between ferritic steels and austenitic stainless steels suffer from a mismatch in coefficients of thermal expansion (CTE) and the migration of carbon during service from the ferritic to the austenitic steel. To overcome these, nickel-based consumables are commonly used. The use of a trimetallic combination with an insert piece of intermediate CTE provides for a more effective lowering of thermal stresses. The current work envisages a trimetallic joint involving modified 9Cr–1Mo steel and 316LN austenitic stainless steel as the base materials and Alloy 800 as the intermediate piece. Of the two joints involved, this paper describes the choice of welding consumables for the joint between Alloy 800 and 316LN. Four consumables were examined: 316, 16-8-2, Inconel 82 and Inconel 182. The comparative evaluation was based on hot cracking tests and estimation of mechanical properties and coefficient of thermal expansion. While 16-8-2 exhibited highest resistance to solidification cracking, the Inconel filler materials also showed adequate resistance; additionally, the latter were superior from the mechanical property and coefficient of thermal expansion view-points. It is therefore concluded that for the joint between Alloy 800 and 316LN the Inconel filler materials offer the best compromise.

1. Introduction

For reasons of economy, fossil fuel-fired power plants use chromium–molybdenum ferritic steels in the lower temperature segments and the more oxidation- and creep-resistant stainless steels in zones of higher temperature. The use of the former in fast breeder nuclear reactors is additionally justified by their resistance to stress corrosion cracking and to corrosion in caustic media. Transition joints between ferritic and austenitic steel tubing thus become necessary because they provide a compromise between operating temperature limitations for the low-alloy grades and the high cost of the stainless steels. Several problems arise in the use of such dissimilar metal welds: cyclic thermal stresses due to differences in coefficient of thermal expansion (CTE) between the dissimilar base materials, preferential stress-oxidation at the weld metal/ferritic steel interface and accelerated creep in a narrow carbon-denuded region on the ferritic steel side caused by the migration of carbon across the interface into the austenitic steel [1–3]. Although in the beginning austenitic stainless steel welding consumables were used, laboratory test results and service experience showed that considerable improvement in performance could be achieved by using nickel-based filler materials [4–9]. The latter have a CTE lying between those of the ferritic and austenitic base metals; carbon diffusion is also significantly retarded because of the reduced carbon activity gradient between ferritic steel and nickel-alloy weld metal, and the low diffusivity of carbon in the nickel-based alloy [3]. This led to the widespread use of nickel-based filler materials for such welds, but even with these joints service failures have been reported [6,7,9,10]; these have been attributed to

* Corresponding author.

0022-3115/00/$ - see front matter
PII: S0022-3115(99)00275-5

the formation and eventual linking-up of creep voids associated with arrays of alloy carbide precipitates in the ferritic steel close to the weld interface [9].

Another approach for improving the life of the transition joints is to use a trimetallic combination with an insert piece made of a material having a CTE intermediate between those of the ferritic and austenitic steels. This would result in a more gradual transition in the CTE and hence in a lower magnitude of stresses during temperature fluctuations occurring in service [11]. One such intermediate material is Alloy 800 and King et al. [11] who suggested it have shown that a considerable reduction in cyclic thermal stress could result from its use. Additionally, Alloy 800 has a high resistance to creep and oxidation at elevated temperatures [12].

The current work envisages a trimetallic transition joint involving modified 9Cr–1Mo steel (P91/T91) and austenitic stainless steel of AISI Type 316LN as the base materials, and Alloy 800 as the intermediate piece. The P91 material is a 9Cr–1Mo steel modified by the addition of vanadium, niobium and nitrogen; with its high-temperature strength improved by precipitation-hardening, it combines creep properties superior to low-alloy steels with physical properties similar to other ferritic alloys, and is used in the higher-temperature steam generator modules [13]. The 316LN austenitic stainless steel is employed as structural material for fast breeder reactors on account of its high creep strength and compatability with liquid sodium. Two joints are thus necessary: one between P91 and Alloy 800, and the other between Alloy 800 and 316LN. While for the former the nickel-based Inconel 82/182 is commonly recommended as welding consumable [11], for the Alloy 800-316LN weld there is a choice of filler materials. The present paper is concerned with this latter aspect.

The candidate filler materials for the joint between Alloy 800 and 316LN are the iron-based austenitic and nickel-based consumables. The relative merits of using various austenitic fillers corresponding to Types 309, 312, 347 and 16-8-2 (16%Cr–8%Ni–2%Mo) were evaluated by King et al. [11]. The main problem encountered was hot cracking, to which Type 347 was the most susceptible and 16-8-2 the least. Type 312 showed little cracking but it contained a relatively large amount of delta ferrite which could transform to embrittling phases during high-temperature service. Bhaduri et al. [14,15] made a comparative study of 16-8-2 with Inconel 82/182 consumables for the joint between Alloy 800 and AISI 304 stainless steel. It was found that 16-8-2 exhibited a lower tendency for microfissuring than Inconel 82/182, but was inferior to the latter in all-weld tensile testing over a range of temperatures. However, transverse weld strengths of joints produced with 16-8-2 filler were only marginally lower and it was therefore considered that 16-8-2 should be preferred for this joint. An additional merit was claimed for 16-8-2, viz., a CTE lying between those of Alloy 800 and 304 stainless steel. The current investigation is concerned with the joint between Alloy 800 and austenitic stainless steel 316LN, the objective being to select the most appropriate filler material based on a comparative evaluation of four consumables, viz., the austenitic stainless steels 316 and 16-8-2 and the nickel-based alloys Inconel 82 and Inconel 182.

2. Experimental

The base materials used in the study were 12 mm thick plates of 316LN and Alloy 800, both of which were in the solution-annealed condition. The four consumables examined were 316 and Inconel 182 (manual metal arc electrodes) and 16-8-2 and Inconel 82 (gas tungsten-arc filler wires). The chemical compositions of the base materials and the undiluted filler materials are given in Table 1. Welding consumable optimisation was based on tests for the following: hot cracking susceptibility, tensile properties, hardness, notch toughness and CTE.

Hot cracking was studied both with longitudinal Varestraint testing for comparing the filler materials and by double fillet weld testing [16] which is sometimes used as an acceptance criterion. Prior to Varestraint testing, welded joints were made between the base materials

Table 1
Chemical composition of materials used (wt%)

Element	Base materials		Undiluted filler materials			
	316LN	Alloy 800	316	16-8-2	Inconel 182	Inconel 82
C	0.02	0.09	0.052	0.07	0.05	0.015
Si	0.3	0.7	0.6	–	0.5	0.1
Mn	1.8	1.0	1.7	1.5	7	2.8
Ni	12.1	31.8	11.5	8.8	69	72.6
Cr	17.9	19.9	18.6	16.2	15	19.6
Mo	2.4	–	2.2	1.6	–	–
Ti	–	0.36	0.04	–	0.1	0.37
Nb	–	–	0.01	–	2	2.68
Fe	Balance	Balance	Balance	Balance	Balance	Balance

using each of the four filler materials, employing a double-V groove edge preparation with an included angle of 75°. The welded pads were sliced into two pieces parallel to the plane of the plates and machined into strips, with the weld metal located along the longest dimension and at the centre of the width. Laboratory scale specimens of dimensions $125\times25\times3$ mm^3 were then prepared for Varestraint testing.

Hot cracking susceptibility of the various weld metals was tested on a moving torch Varestraint hot cracking test device, model LT 1100. During the test an autogenous gas tungsten-arc weld bead was deposited on the original weld metal as shown in Fig. 1 and solidification cracking was induced by applying a predetermined bending strain through a pneumatically activated ram forcing the sample to conform to the radius of a die block. The augmented bending strain e applied to the surface of the test specimen is related to the radius of the die block by the equation $e = t/2R$, where t is the specimen thickness and R is the radius of the die block. The strain levels applied were 0.5%, 1%, 2% and 4%. For each weld metal, eight specimens were tested at 4% strain and three each at the lower strain levels. The welding parameters used during Varestraint testing were kept constant as follows: current = 100 A, voltage = 11.5 V and travel speed = 4.2 mm/s. Following testing, the specimens were examined at a magnification of 60 using a stereomicroscope for measuring crack length. Both total crack length (TCL) and maximum crack length (MCL) were used as criteria for evaluating the hot cracking susceptibility of the weld metals.

The double fillet weld test, prescribed under the specification DIN 50129, is for assessing the liability to cracking of filler materials and is particularly applicable in the case of dissimilar metal welds [16]. The testing arrangement is shown in Fig. 2. The base plate was the lower-alloy parent metal, in the present case the 316LN steel, and the web was made from Alloy 800. For increasing restraint, ribs were attached to the base plate as shown. Fillet welds 1 and 2 were then deposited in the downhand position using the filler material under test. The specification calls for weld 1 to be made with thickness equal to about 5 mm and weld 2 with a

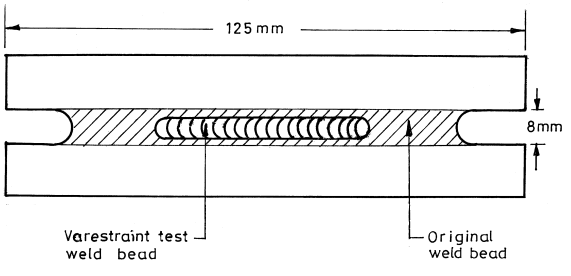

Fig. 1. Specimen with weld bead for Varestraint testing.

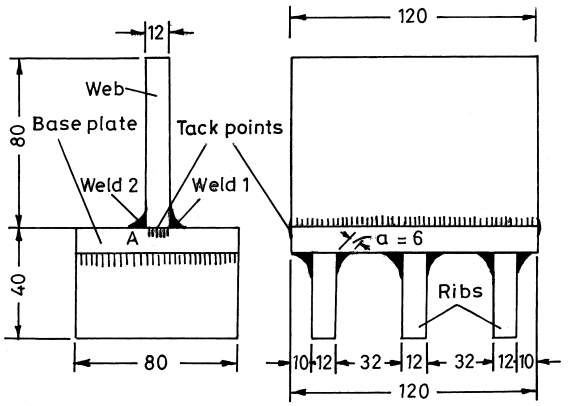

Fig. 2. Specimen for double fillet weld test (dimensions in mm).

thickness of about 4 mm. At the end of the test, the weld 2 is to be examined for surface cracks at a magnification of about 6×. Subsequently the weld 1 is removed by machining, and weld 2 broken open by bending the web from the root for detecting root cracks if any. The filler material is acceptable if no cracks are found. This test was performed for each of the four filler materials under study.

Transverse sections of the welds were metallographically characterised after electrolytic etching in 10% oxalic acid. In one case, Murakami's etch was used for revealing ferrite and in another electrolytic etching with 10% NaOH was done to reveal the sigma phase.

For mechanical testing, weld pads were prepared as before but with single-V groove edges with an included angle of 60° so that sufficient weld metal cross-section would be available for longitudinal all-weld tensile testing. Button-head type cylindrical all-weld and transverse tensile specimens (28.6 mm gauge length and 4 mm gauge diameter) were tested at a nominal strain rate of 2.4×10^{-4}/s at room temperature. Transverse tensile specimens (length perpendicular to welding direction) were also produced and tested both at room temperature and at 550°C.

Microhardness measurements were made across the weld metals at a load of 500 g using a Shimadzu microhardness tester.

Room-temperature toughness of the welds was determined using standard $55\times10\times10$ mm^3 Charpy V-notch impact specimens. In accordance with the design requirements for qualifying welding consumables [17] for fast breeder reactor service, weld metal specimens were also tested for notch toughness after subjecting them to an embrittling heat treatment at 750°C for 100 h. The fractured faces were examined in a JEOL scanning electron microscope.

The coefficients of thermal expansion of the two base materials and the four undiluted filler materials were

determined by the dilatation method in a thermomechanical analyser, model Mettler TA3000.

3. Results and discussion

3.1. Microstructures

Fig. 3(a) shows the microstructure of the weld metal made with 316 electrode. The substructure is seen to be dendritic with well-developed side-branches. The bulk of the fusion zone was observed to have solidified in the fully austenitic mode, but occasionally it showed austenitic/ferritic (AF) and ferritic/austenitic (FA) modes of solidification, as illustrated in Fig. 3(b). The interface (Fig. 3(c)) of the weld with the 316LN base metal reveals the presence of an unmixed zone in which the base metal has melted and resolidified without mixing with the filler material; here also, more ferrite can be detected than in the bulk weld metal. On the base metal side there is evidence of grain boundary thickening and liquation, especially where inclusion-rich stringers intersect the fusion boundary. The interface of the weld metal with Alloy 800 also shows an unmixed zone and evidence of grain boundary liquation (Fig. 3(d)). The tendency for Alloy 800 base metal to liquate at the HAZ grain boundaries is greater apparently due to the presence of titanium which is known to cause liquation cracking in the HAZ in materials similar to Alloy 800 [18].

In contrast to the above, the weld metal produced with 16-8-2 filler metal exhibits a fully cellular substructure as shown in Fig. 4(a). This weld metal also is predominantly fully austenitic, except for the region near the root of the weld (Fig. 4(b), prepared with

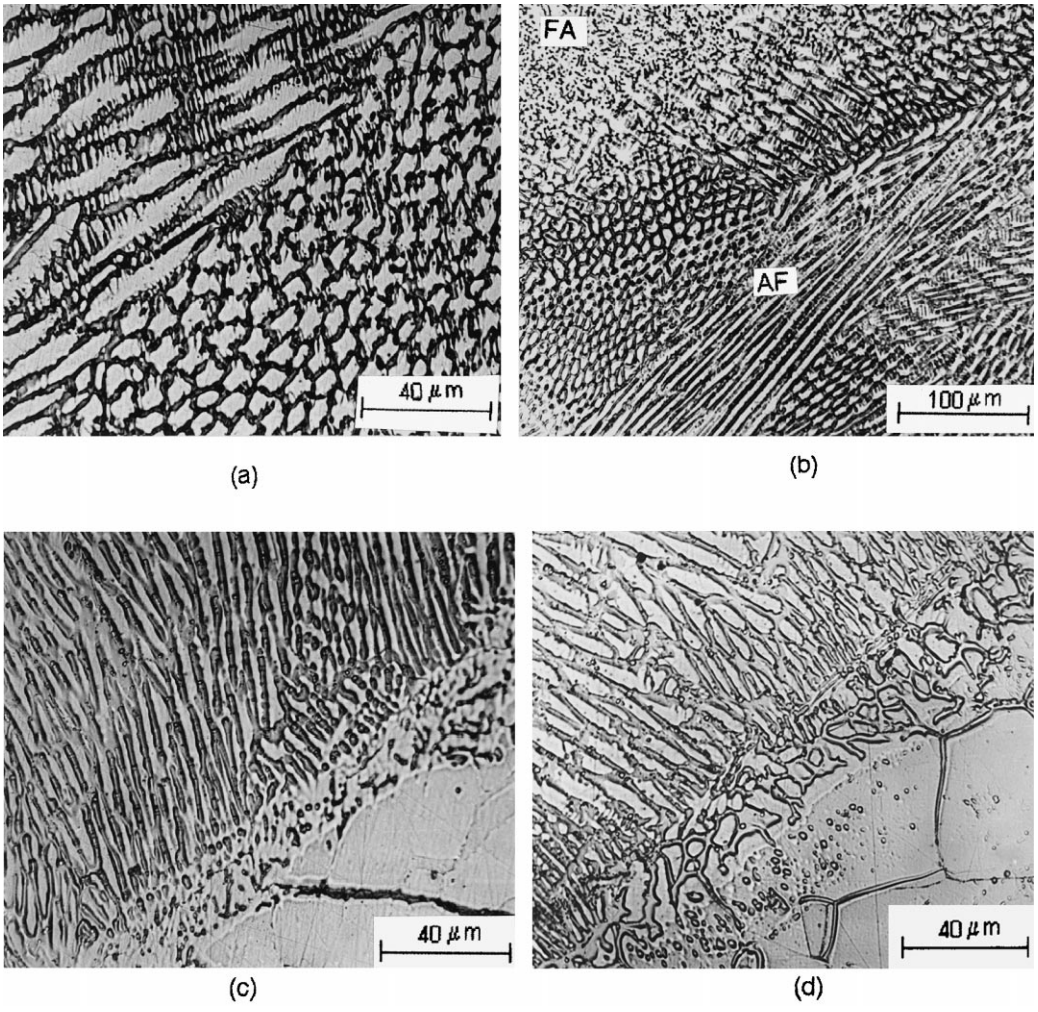

Fig. 3. Weld metal made with 316 electrode: (a) interior of weld, (b) 316 weld metal showing regions of AF and FA modes of solidification, (c) interface with 316LN base metal, and (d) interface with Alloy 800 base metal.

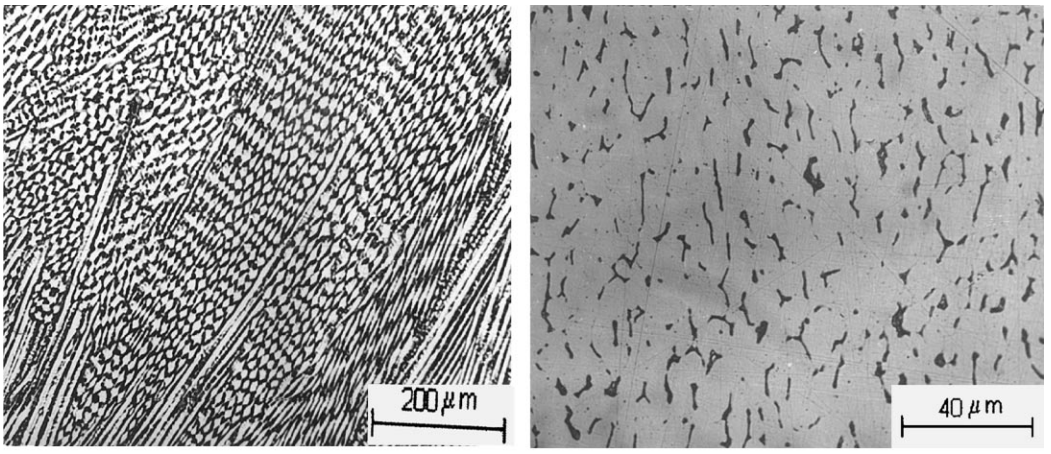

Fig. 4. Weld metal with 16-8-2 filler wire: (a) interior of weld, (b) region near root of weld showing intercellular ferrite.

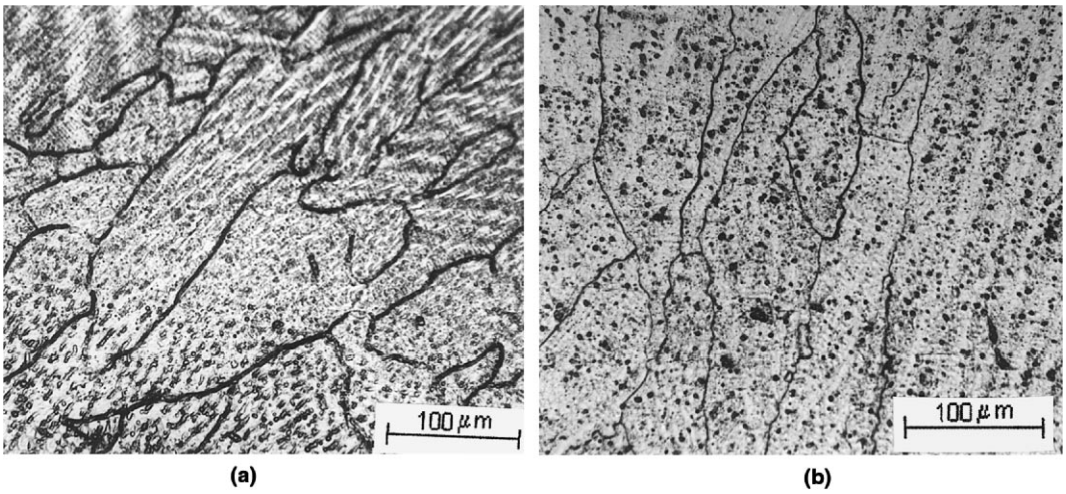

Fig. 5. (a) Weld metal produced with Inconel 82 filler wire, (b) weld metal produced with Inconel 182 electrode.

Murakami's reagent) and the region adjoining the 316LN base metal where some ferrite has been formed on account of dilution effects.

The microstructures of Inconel 82 and Inconel 182 weld metals are shown in Fig. 5(a) and (b). The microstructure are very similar to each other except that the Inconel 182 fusion zone deposited by manual metal arc welding contains a large number of fine inclusions. It may be noted in Fig. 5(a) that the weld metal shows recrystallised features with extensive grain boundary migration that cuts across the cellular solidification structure.

3.2. Hardness survey

The hardness variations across the welds are shown in Fig. 6. Since the behaviour with Inconel 82 and Inconel 182 was very similar, only the results with Inconel 182 are presented. The welds in all cases exhibit a hardness greater than those of the two base materials, even when austenitic stainless steel filler materials have been used. This is primarily to be attributed to the slightly increased carbon content in the weld metals made with 16-8-2 and 316 filler materials. While the 316LN base material has a carbon content of 0.02 wt% the two filler materials have carbon contents of 0.07 wt% (16-8-2) and 0.052 wt% (316). It may also be noticed that in all cases there is a gradual, though slight, increase in hardness in the weld metal on traversing from the 316LN to the Alloy 800 side. This suggests that despite the convection effects in the weld metal there could be a grading in composition on account of dilution from the two different base materials.

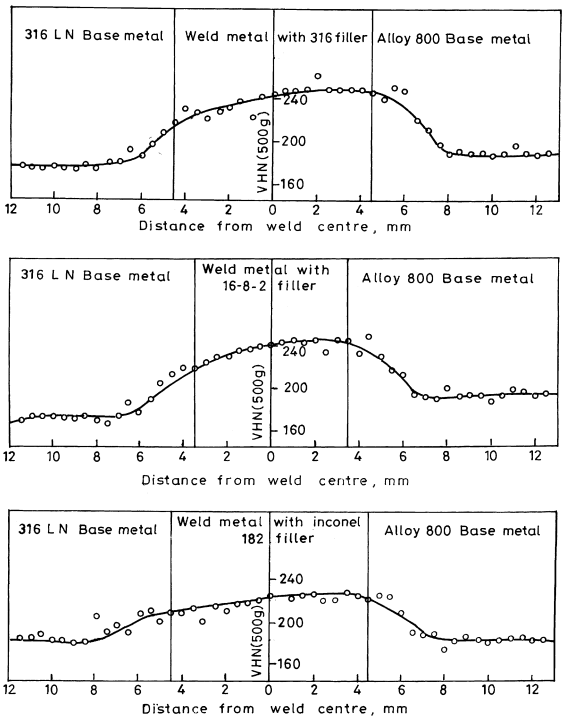

Fig. 6. Hardness profile across the welds produced with different filler materials.

3.3. Hot cracking susceptibility

3.3.1. Varestraint tests

The results of the longitudinal Varestraint testing are given in Fig. 7(a) and (b) which show the dependence of total crack length and maximum crack length, respectively, on the applied strain. It is clear from both the plots that the 16-8-2 weld metal shows the least susceptibility to hot cracking. The occasional anomalous behaviour observed in some cases may be attributed to the nature of producing the specimens for testing. While in the conventional Varestraint testing wrought base metal specimens are directly used, in the current investigation weld metals were first produced using the respective filler materials and these were remelted during the Varestraint testing. Minor variations in dilution at the region of strain application might have caused the observed behaviour. In Fig. 7(a) it may be noticed that all four weld metals show finite cracking even at 0.5% strain signifying the absence of any threshold strain. It may be observed in Fig. 7(b) that the maximum crack length in the 16-8-2 weld metal does not increase when the strain is increased from 2% to 4%, thus revealing a saturation effect at 2% strain. While both Inconel 82 and Inconel 182 weld metals exhibit a greater degree of cracking than 16-8-2, there is only a marginal difference between Inconel 82 and Inconel 182.

The microstructures of the cracked regions are shown in Fig. 8(a)–(f). The cracking is seen to be predominantly intergranular; some cracks along substructure boundaries can also be observed. The more extensive cracking in 316 weld metal (Fig. 8(a)) may be a result of its predominantly austenitic mode of solidification and pronounced dendritic morphology. It is known that dendritic structures are associated with greater segregation and are more prone to cracking. Many cracks exhibited backfilling as shown in Fig. 8(b). It is of interest to note that the backfilled regions

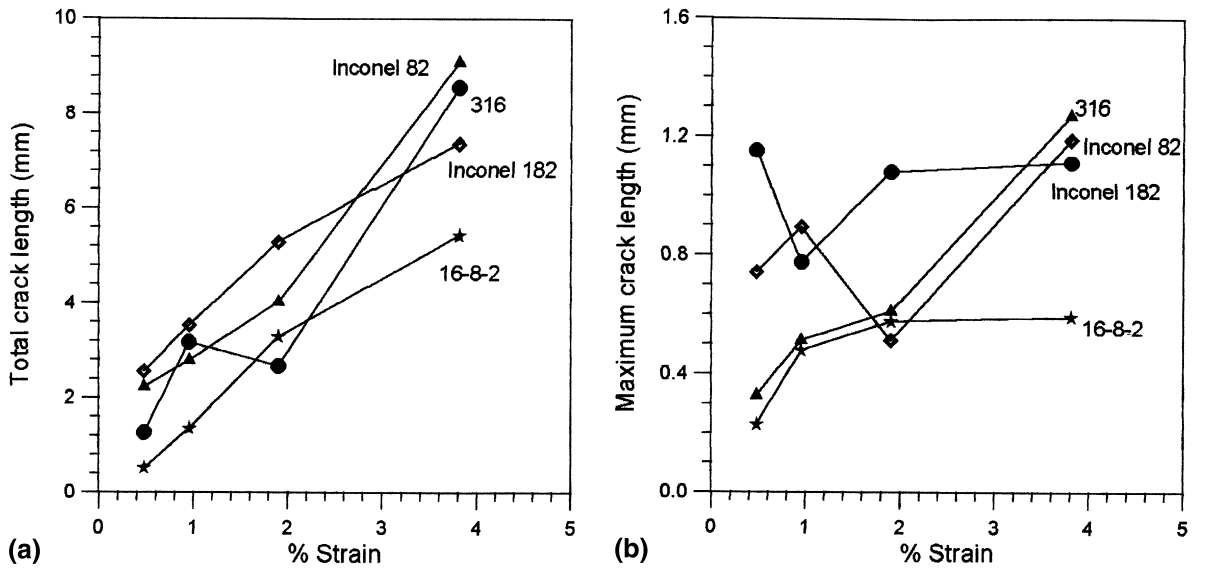

Fig. 7. (a) Total crack length in fusion zone for the four weld metals, (b) maximum crack length in fusion zone for the four weld metals.

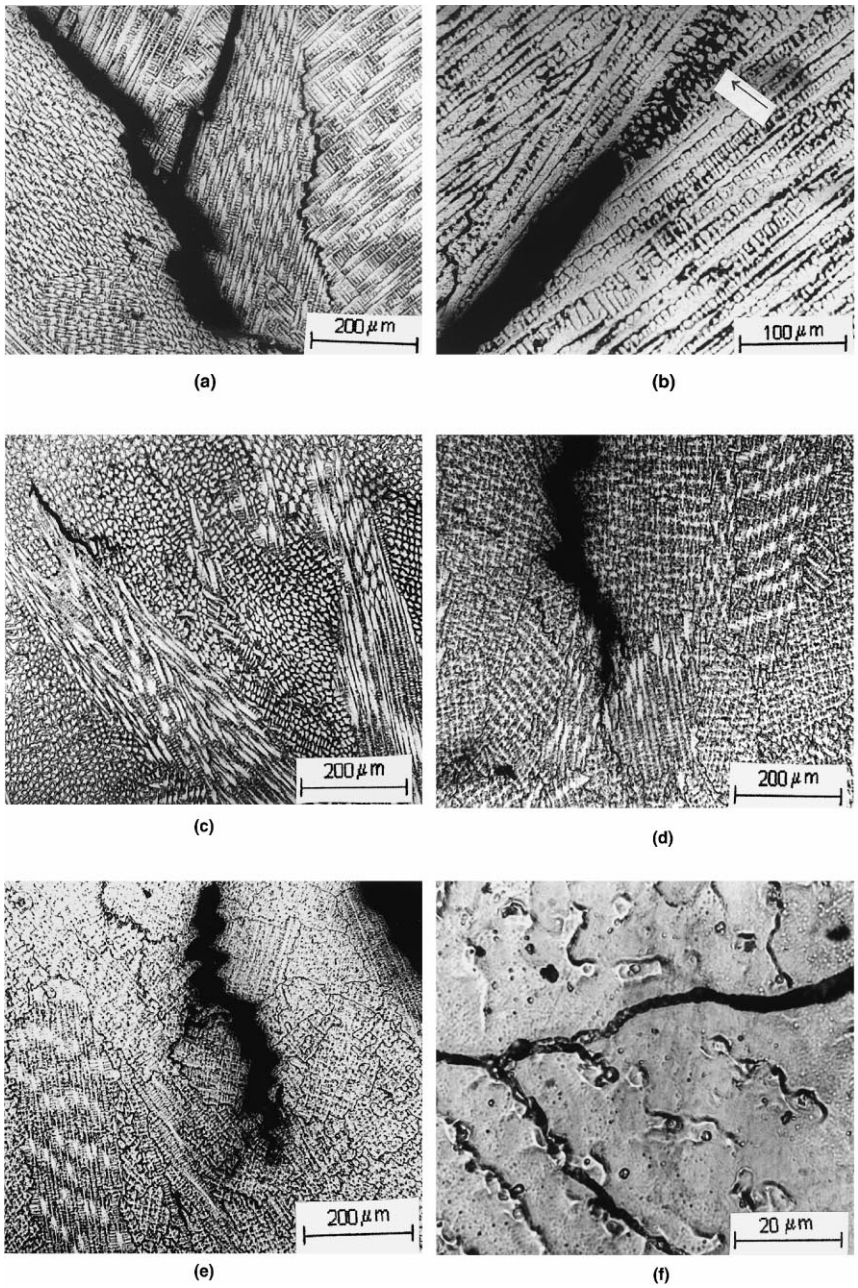

Fig. 8. (a) Solidification cracking in 316 weld metal, (b) solidification crack in 316 weld metal showing back-filled region (arrow) with ferrite enrichment, (c) solidification cracking in 16-8-2 weld metal, (d) solidification cracking in Inconel 82 weld metal, (e) solidification cracking in Inconel 182 weld metal, and (f) solidification cracking in Inconel 182 weld metal showing Laves phase along grain boundaries and crack extensions.

show a higher ferrite content than in the general microstructure which may be attributed to the enrichment of ferrite stabilisers in the liquid during primary austenitic solidification.

The more cellular mode of solidification in 16-8-2 weld metal is seen to have resulted in less extensive and finer cracking (Fig. 8(c)), even though no intercellular ferrite is present except in isolated locations. The cracking in Inconel 82 (Fig. 8(d)) and in Inconel 182 (Fig. 8(e)) is similar and the crack tip is much sharper than in the previous cases. Also, both showed evidence of extensive Laves phase formation along grain boundaries,

intercellular regions and crack extensions, as seen for example in Fig. 8(f).

3.3.2. Double fillet weld tests

The hot cracking resistance was also evaluated by the double fillet weld test specified under DIN 50129. This test was performed on welds made with each of the four consumables in accordance with the procedure described earlier. After the welds were completed, dye penetrant testing failed to reveal surface cracks in any of the four welds tested. The test also prescribes the removal of run 1 by machining and the breaking open of the test run by bending the web from the root in order to examine the root cracks. This procedure also did not reveal any root crack in any of the four filler materials tested.

The double fillet weld test is essentially an acceptance test which is particularly suited for assessing dissimilar metal welds. It is significant that even under the high degree of restraint imposed in this test no surface or root cracks formed in any of the four welds, so that, in accordance with the specification, all the four filler materials are to be considered acceptable. The difference in results between the double fillet weld test and the Varestraint test can be shown to arise from the differences in strain rates experienced during testing. Matsuda and Tomita [19] have shown, by direct observation of cracking on specimens strained at various rates during welding, that high strain rates tend to amplify differences in cracking behaviour among different materials. Hence, the Varestraint test, which employs an externally imposed strain at a high strain rate, is quite sensitive even to minor differences in cracking susceptibility. The double fillet weld test, on the other hand, is a self-restraint test characterised by an inherently lower strain rate. While as a result the double fillet weld test is less sensitive in grading different materials, it does give a definite and reliable acceptance criterion; this is because it represents a better simulation of practical welding situations and also because the joint design in the test is such that severe conditions due to the notch effect at A (see Fig. 2) are imposed on the solidifying test weld.

3.4. Tensile properties

The results of transverse tensile tests both at room temperature and at 550°C are listed in Table 2. In the case of room-temperature properties, while the joints made with 316 and 16-8-2 filler materials exhibited fusion zone failure, the weldments with Inconel 82 and Inconel 182 filler materials failed in the weaker parent metal, i.e., 316LN. The parent metal failures exhibited a greater reduction in area than the weld metal failures. The most significant result from these tests is that Inconel 82/Inconel 182 filler material is superior to 316 and 16-8-2 filler metals in tensile behaviour.

Regarding the tensile properties determined at 550°C, there is an understandable drop in yield strength and ultimate tensile strength in all cases. Concerning ductility, however, while there was no significant change in the tensile elongation in the case of weldments produced with the stainless steel fillers, a significant decrease in elongation and reduction in area was noticed for the

Table 2
Tensile properties of transverse specimens at room temperature and at 550°C

Filler metal	Yield strength (MPa)	Ultimate tensile strength (MPa)	Total elongation (%)	Reduction in area (%)	Location of failure
316 (RT[a])	275	537	26	50	Weld
316 (550°C)	264	428	20	57	Base metal
16-8-2 (RT)	301	530	25	53	Weld
16-8-2 (550°C)	258	430	27	58	Weld
Inconel 182 (RT)	312	613	30	72	Base metal
Inconel 182 (550°C)	275	437	16	55	Base metal
Inconel 82 (RT)	333	630	36	75	Base metal
Inconel 82 (550°C)	280	430	20	59	Base metal

[a] Room temperature (RT).

Table 3
Tensile properties of longitudinal all-weld specimens

Filler metal	Yield strength (MPa)	Ultimate tensile strength (MPa)	Total elongation (%)	Reduction in area (%)
316	301	525	39	54
16-8-2	359	578	42	52
Inconel 182	388	672	32	46
Inconel 82	391	634	37	57

joints made with Inconel filler materials. An important point to note in this connection is that in all specimens produced with Inconel consumables the failure in the high-temperature test occurred in the base metal (316LN). In the current program of work the tensile properties of the Inconel weld metals were not determined at 550°C using all-weld specimens. However, it has been shown in an earlier investigation [15] that Inconel weld metal exhibited much higher strength in all-weld tensile testing at 500°C than 16-8-2 weld metal. In the current work also, as described below, longitudinal all-weld tensile testing at room temperature has confirmed the higher strength of Inconel weld deposits in relation to the stainless steel weld metals. It is clear therefore that Inconel shows higher strength than either 316 or 16-8-2 both at room temperature and at elevated temperature.

The reduced ductility measured at 550°C in joints made with Inconel filler materials can now be explained. Because of the difference in strengths noted above, deformation during the tensile test is confined almost entirely to the softer austenitic base metal which eventually necks down to final rupture. The constraining effect of the weld metal of significantly higher strength adjacent to the region of necking makes strain accommodation difficult and reduces the total elongation. Such constraint-induced low ductility during tensile testing has also been reported for tensile fracture occurring in the carbon-depleted soft zone of post-weld heat-treated dissimilar welds between two different Cr–Mo steels [20]. The room-temperature ductility is higher for these joints because the difference in strength between weld and base metals is not as large as at 550°C.

Since some weldments failed as above in the weld metal and some others in the base metal, it was considered that a better comparison of filler materials would be possible with longitudinal all-weld tensile testing. These data, determined only at room temperature, are listed in Table 3. These reveal the decided superiority of the nickel-based filler materials from the strength point of view. Also, although the use of the two stainless steel fillers is seen to result in a greater degree of ductility than

Table 4
Charpy V-notch impact energy at room temperature

Material	Impact energy (J) (as-welded condition)	Impact energy (J) (after aging 750°C, 100 h)
Type 316LN stainless steel (base metal)	161	–
Alloy 800 (base metal)	155	–
316 weld metal	129	45
16-8-2 weld metal	146	107
Inconel 182 weld metal	119	100
Inconel 82 weld metal	158	137

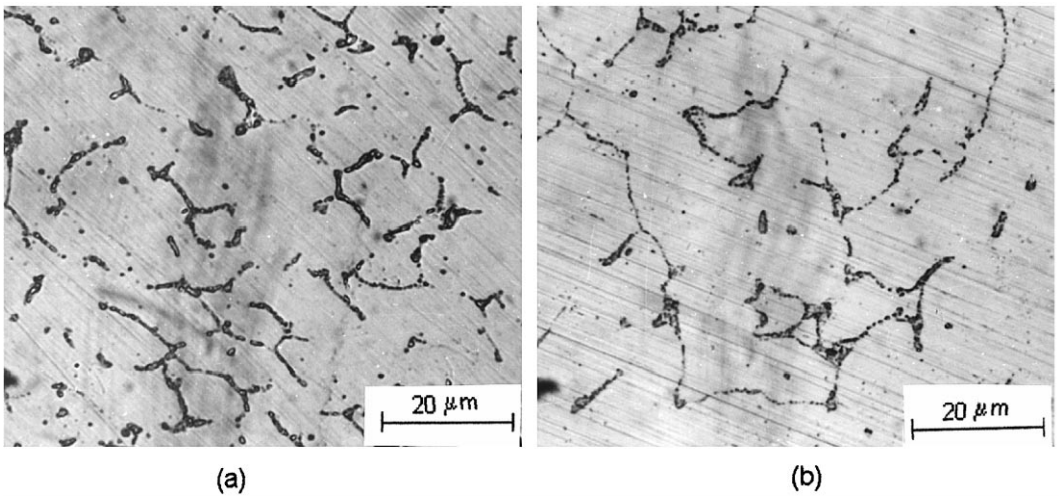

Fig. 9. Sigma phase formation in stainless steel weld metal after aging for 100 h at 750°C: (a) aged 316 weld metal, (b) aged 16-8-2 weld metal.

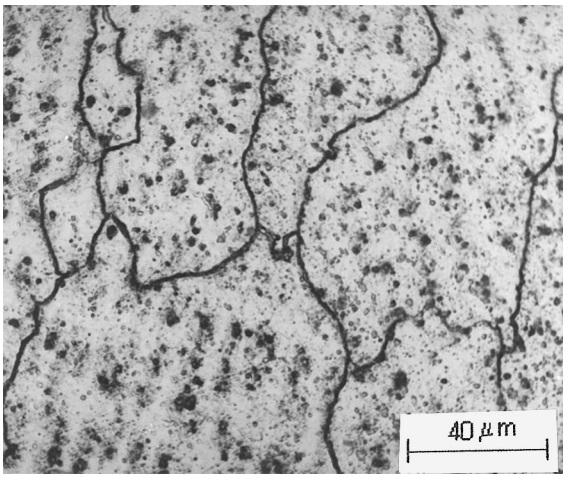

Fig. 10. Microstructure of Inconel 182 weld metal after aging for 100 h at 750°C.

with the nickel-base fillers, the difference between them is not considerable. Between Inconel 82 and Inconel 182, the latter shows a slightly lower ductility, probably owing to its higher inclusion content resulting from the use of manual metal arc welding.

3.5. Notch toughness

The Charpy test results both for as-welded and aged conditions are listed in Table 4. The base metal toughness values are also included for comparison. In the as-welded condition, all four weld metals exhibit toughness values which are not much lower than for the two base metals. Also, all the four exceed the minimum prescribed value of 80 J under the fast breeder reactor specification for the qualification of such dissimilar joints [21]. Between Inconel 82 and Inconel 182, the former exhibits much greater toughness which clearly appears to be due to its lower inclusion content in relation to Inconel 182. On the other hand, the aging treatment (750°C, 100 h) is

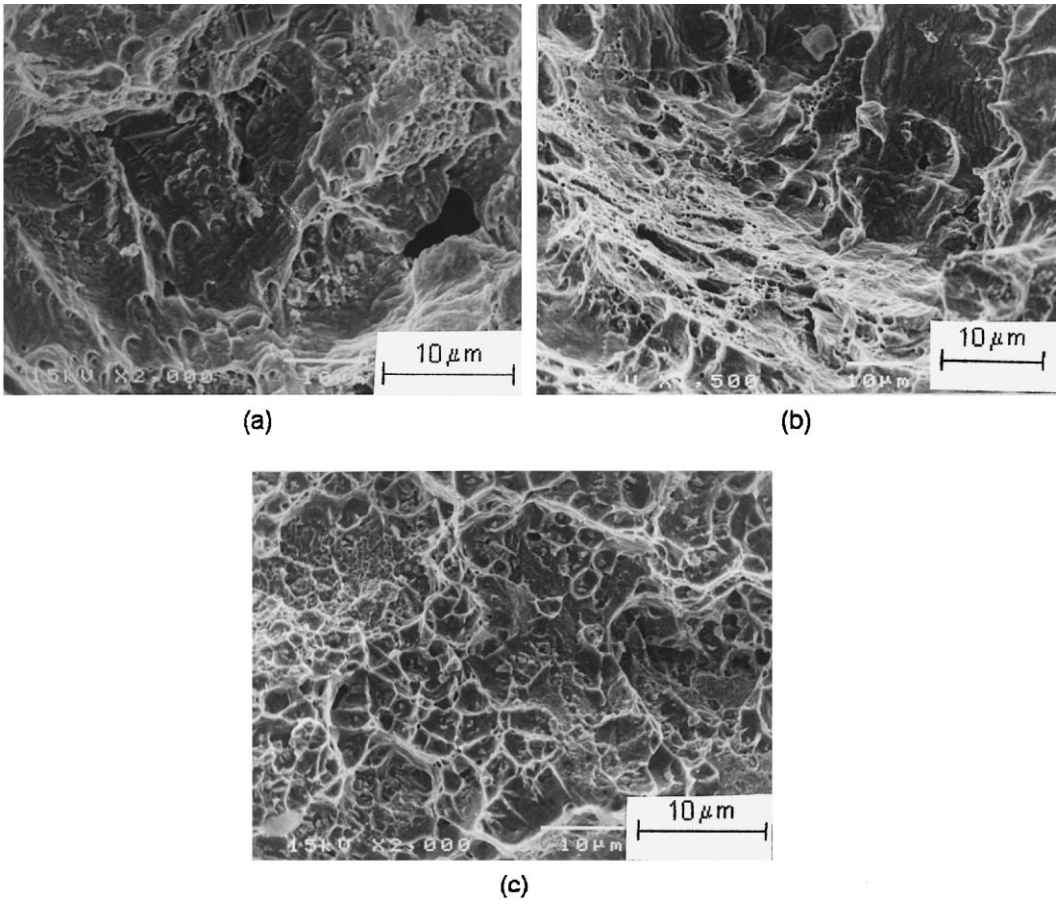

Fig. 11. SEM fractographs of fractured Charpy impact specimens: (a) aged 316 weld metal, (b) aged 16-8-2 weld metal, and (c) aged Inconel 182 weld metal.

seen to reduce the toughness in the case of the two stainless steel filler materials and the reduction is quite drastic when 316 electrode is used. This can be explained in terms of the microstructures of the two aged weld metals given in Fig. 9(a) and (b) (prepared by electrolytic etching in 10% NaOH). These reveal the presence of a discontinuous network of the sigma phase and fine carbide particles. Part of the sigma phase is seen to have formed in spheroidal fashion. Between the two stainless steel weld metals, a greater proportion of the sigma phase can be seen in Fig. 9(a) corresponding to 316 filler material. The sigma phase and carbide particles have formed in the place of ferrite that was originally present in the interdendritic regions in the as-welded structures. The high-temperature aging has obviously resulted in the transformation of the ferrite to these phases. The greater degree of sigma formation observed in the 316 weld metal than in 16-8-2, is consistent with the lower toughness of the former in the aged condition. However, both weld metals still retain significant toughness due to the low original ferrite content and a spherodised morphology of the sigma phase. On the other hand, in the case of the two nickel-based consumables, the lowering of toughness consequent to aging is much less significant. This is also borne out by the absence of any kind of precipitation in the micrograph of Inconel 182 weld metal after the aging treatment shown in Fig. 10. In an earlier investigation on the behaviour of nickel-based weld metal during heat treatment in the 600–900°C temperature range [22], embrittling precipitation was found to occur at 700°C, but only after aging for 10 000 h. Precipitation and toughness loss were less pronounced at 600°C, and even less in the range 800–900°C. It is therefore not surprising that in the current work the two nickel-based weld metals did not exhibit serious toughness reduction on aging for 100 h at 750°C. This clearly shows the greater thermal stability of the nickel alloy filler materials in relation to the stainless steel consumables.

The Charpy test fracture surfaces of the aged weld metal specimens were examined in the scanning electron microscope. The fractographs are reproduced in Fig. 11(a)–(c). While the aged weld metals made with the two stainless steel fillers exhibit regions of cleavage fracture as seen in Fig. 11(a) and (b), the fusion zone in the case of aged Inconel 182 (Fig. 11(c)) filler material reveals a fully ductile fracture.

3.6. Coefficient of thermal expansion

The coefficients of thermal expansion of the base materials and undiluted filler materials are plotted in Fig. 12 as a function of temperature, in the temperature range 50–610°C. The CTE values of the two austenitic stainless steel fillers are understandably close to that of the 316LN base metal and the curves for all the three lie well above the curve for Alloy 800 base metal. On the other hand, the Inconel filler materials exhibit CTE values that lie between those of the two base materials. In particular, Inconel 182 is seen to bridge the gap between 316LN and Alloy 800 most satisfactorily. Considering the possibility of thermal fluctuations during service, the Inconel filler materials, especially Inconel 182, therefore appear to be better suited than the stainless steel consumables.

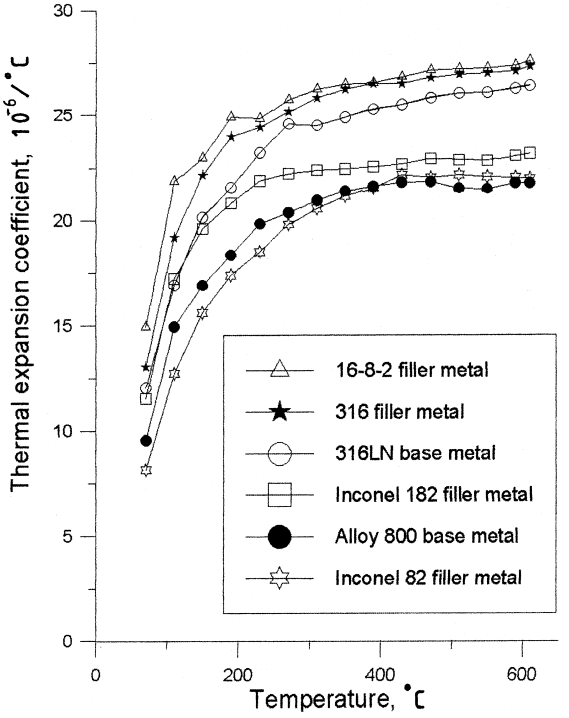

Fig. 12. Coefficients of thermal expansion of base and filler materials.

4. Conclusions

From the results of the various tests, it is clear that the nickel-based consumables produce welds exhibiting better tensile properties and improved thermal stability in relation to the austenitic steel filler materials. The absence of microstructural deterioration at high temperatures is considered particularly important in view of the usual operating conditions for these joints. From a consideration of thermal expansion coefficients also, the Inconel filler materials are seen to be superior to the stainless steel consumables. The Varestraint testing has shown, on the other hand, that the 16-8-2 filler material results in the lowest susceptibility to solidification cracking. However, as discussed earlier, the double fillet weld tests have confirmed that all the weld metals

including those produced with the nickel-alloy filler materials do indeed exhibit hot cracking resistance adequate for reasonably severe restraint conditions expected in service. In the final analysis, therefore, it may be concluded that, for joints between 316LN stainless steel and Alloy 800, Inconel 82/182 filler materials offer the best compromise.

Acknowledgements

The work described in this paper is part of a project (Sanction No: 36/7/96-R&D-ii) sponsored by the Board of Research in Nuclear Sciences, Department of Atomic Energy. The authors wish to acknowledge the financial assistance provided by them.

References

[1] C.D. Lundin, Welding J. 61 (1982) 58s.
[2] K.G.K. Murti, S. Sundaresan, Welding J. 64 (198s) 327s.
[3] R. Viswanathan, in: Proceedings of the AWS/EPRI Conference on Joining Dissimilar Metals, Pittsburgh, PA, 1982, pp. 7–27.
[4] R.D. Nicholson, Metals Technol. 9 (1982) 305.
[5] W.K.C. Jones, Welding J. 43 (1974) 225s.
[6] P.E. Haas, in: Proceedings of the AWS/EPRI Conference on Joining Dissimilar Metals, Pittsburgh, PA, 1982, pp. 37–47.
[7] A.T. Price, in: Proceedings of the AWS/EPRI Conference on Joining Dissimilar Metals, Pittsburg, PA, 1982, pp. 48–79.
[8] David N. French, Welding Design Fabricat. 1984 (May), 92.
[9] R.D. Nicholson, Met. Technol. 11 (1984) 115.
[10] K.H. Holko, C.C. Li, in: Proceedings of the Conference on Welding Technology for Energy Applications, Gatlinburg, TN, 1982, pp. 641–672.
[11] J.F. King, M.D. Sullivan, G.M. Slaughter, Welding J. 56 (1977) 354s.
[12] W.B. Jones, R.M. Allen, Metall. Trans. A 13 (1982) 637.
[13] Atsuro Iseda et al., Sumitomo Res. 36 (1998).
[14] A.K. Bhaduri et al., Mater. Sci. Technol. 4 (1988) 1020.
[15] A.K. Bhaduri et al., Int. J. Press. Ves. Piping 58 (1994) 251.
[16] DIN specification 50129. Testing of Metallic Materials. Testing of Welding Filler Metals for Liability to Cracking, October 1973.
[17] PFBR/32040/SP/1002/R-0 – Prototype Fast Breeder Reactor specification for the qualification of the welding consumables as proposed by IGCAR, Kalpakkam, India.
[18] J.A. Brooks, Welding J. 53 (1974) 517s.
[19] Fukuhisa Matsuda, Shigo Tomita, IIW IX-1708-93.
[20] S.K. Albert, G. Srinivasan, T.P.S. Gill, in: Proceedings of the National Welding Seminar, Bangalore, India, 1997, pp. 222–232.
[21] PFBR/33700/SP/1008/R-0 – Prototype Fast Breeder specification for the qualification of the joint between 316LN austenitic stainless steel and Alloy 800 as proposed by IGCAR, Kalpakkam, India.
[22] J.O. Nilsson, B. Lundquist, M. Lonnberg, Welding J. 73 (1994) 45.